polymers

MDPI

Article

Incorporation effect of low molecular weight poly(mannitol sebacate)s on PLA electrospun fibers

V. Hevilla [1,2], A. Sonseca [3], E. Gimenez [3], C. Echeverría [1,2], A. Muñoz-Bonilla [1,2] and M. Fernández-García [1,2,*]

[1] Instituto de Ciencia y Tecnología de Polímeros (ICTP-CSIC), C/Juan de la Cierva, 3, Madrid 28006, Spain
[2] Interdisciplinary Platform for "Sustainable Plastics towards a Circular Economy" (SUSPLAST-CSIC)
[3] Instituto de Tecnología de Materiales, Universitat Politècnica de València, Camino de Vera, s/n, Valencia 46022, Spain
* Correspondence: martafg@ictp.csic.es

Abstract: We report the synthesis of low molecular weight biobased poly(mannitol sebacate) (PMS) and its functionalization with acrylate groups (PMSAc). These synthesized polyesters were, then, blended at low amount (10 wt%) with poly (lactic acid) PLA to prepare aligned fibers by electrospinning coupled to a rotatory collector. The obtained fibers were extensively studied by Fourier-transform infrared (FTIR), scanning electron microscopy (SEM), differential scanning calorimetry (DSC) and wide angle X-ray diffraction (WAXS) employing synchrotron radiation. The incorporation of the PMSs on the PLA fibers did not affect significantly the fiber diameters whereas the alignment is almost maintained. Crystallinity and thermal properties were also slightly modified with the addition of PMSs, an increase in the degree of crystallinity and the glass transition temperature of the system was observed. Remarkably, PLA/PMSs fibers were more ductile due to the elastomeric character of PMS, with higher values of elongation at break and tensile strength, and smaller Young modulus in comparison with PLA fibers. These modifications of the properties were more noticeable in the case of the acrylated PMS, which also provided readily available functional groups at the surface for further chemical reactions, such as Michael addition or crosslinking processes.

Citation: V. Hevilla; A. Sonseca; E. Gimenez; C. Echeverría; A. Muñoz-Bonilla; M. Fernández-García **Incorporation effect of low molecular weight poly(mannitol sebacate)s on PLA electrospun fibers.** *Polymers* **2022**, *13*, x. https://doi.org/10.3390/xxxxx

Academic Editor(s):

Received: date
Accepted: date
Published: date

1. Introduction

Nowadays, the green deal requires the efficient use of resources and the nature protection, avoiding the contamination and minimizing the carbon foot-print. One of the strategies to address this challenge focuses on the research toward the development of more sustainable materials. This implies the use of sustainable raw materials and also the use of more sustainable processing methods that could contribute to minimize energy expenditure in their production, and the use of low processing temperatures, for example.

Nowadays, one of the most used processing techniques in polymer science and technology is electrospinning [1]. This is an inexpensive and effective process which can produce directly and simply continuous polymer micro- or nanofibers with a 3D topography (scaffolds), high porosity, large surface area, etc. [2][3][4][5][6]. The mechanism behind the fiber obtainment involves the application of an electrostatic force to generate a polymeric jet towards a collector electrode [1]. The obtained fiber properties can be fine-tuned by applying different set-up conditions, different collectors (plate, rotating drum…) and parameters to fulfill the requirements of the desired potential application for the final material. For instance, recent studies demonstrated that the production of aligned electrospun fibers by means of rotating drum gives rise to fiber mats with potential applications in wound healing. This fiber arrangement mimics the extracellular matrix besides of contributing to improve the cell viability compared to random fibers. For all these reasons, electrospun membranes are ideal materials for applications in different areas such as energy storage (supercapacitors) [7], electronic applications (membranes for Li-ion batteries) [7] and in biomedicine [8][9] with particular applicability in tissue engineering [10][11][12].

For the development of sustainable materials, biobased and natural polymers or biopolymers have gained interest in electrospinning processing technique. They are postulated as plausible candidates to substitute fossil fuel derived polymers also providing properties such as biocompatibility and biodegradability. For instance, poly(lactic acid) (PLA) [13] has been extensively studied for biomedical uses, among others. However, this polymer presents drawbacks that limit somehow its use in some bioapplications, such as tissue engineering or tissue regeneration. For instance, PLA is sensitive to temperature and has a low rate of degradation, a poor cellular behavior, a moderate inflammatory response and a low toughness. To overcome some of these problems recent studies have focused the strategy on blending PLA with other materials to improve the mechanical properties and thus, expand the range of applications [14–18]. For this purpose, polyol polyesters are presented as good candidates. These polymers are made from renewable resources, such as glycerol, sorbitol, mannitol and diacids, and can be used also to a large number of applications such as elastomers, sealants, and adhesives, etc. [19–22] They are generally environmentally degradable and, during prolonged contact with tissues, polyol polyesters hydrolyze to their natural building blocks from that are built up [23,24]. Therefore, they are good candidates to improve the physico-chemical characteristics of PLA. Among the polyol polyesters, the family of poly(polyol sebacate)s is probably one of the most appropriate. These polymers present a degradation mechanism that provokes a linear loss of mass and mechanical properties along the process instead of dramatic diminish of properties. Then, the material typically maintains its geometry, performance and stiffness being more compatible with soft tissues [2,3].

Belonging to this family, poly(mannitol sebacate) (PMS) made from mannitol that is a diastereomer of sorbitol (the most well-studied natural polysaccharide-derived hexitol), and sebacic acid (a natural C10 fatty acid) which is directly produced from castor oil. The main problem of its synthesis is the high melting point of mannitol as well as its low solubility in organic solvents, facts for which it is made by melt polycondensation [20]. PMS has been used as upconverting cross-linked elastomer with covalently tethered chromophores [25], but mainly as matrix in blends and nanocomposites with increased modulus and enhanced strain and toughness [14,22,26], which are requirements needed for applications in surgical procedures and tissue engineering [19,20].

In addition to this, PMS has pendant hydroxyl groups on its structure, which can be functionalized with other molecules and therefore, provide new properties to the PMS such as antimicrobial activity and/or antioxidant activity. Thus, the aim of this work is to obtain aligned fibers from the combination of PLA and PMS and the combination of PLA and acrylated PMS (PMSAc) by means of electrospinning coupled to a rotatory collector. Our objective is double, on one hand, to study the effect of the incorporation of PMS and PMSAc in the properties of the obtained fibers, and secondly, to demonstrate the possibility of surface functionalization of PLA/PMSAc fibers as a proof of concept, in order to provide additional functionalities to the fiber mats. The resulting fibers are analyzed in terms of morphology, structural properties and crystallinity, thermal properties, and stability and mechanical properties.

2. Experimental

2.1. Materials

Sebacic acid (SA), mannitol (MA), triethylamine (TEA), acryloyl chloride, hydrochloric acid (HCl), anhydrous N,N-dimethylformamide (DMF), deuterated dimethyl sulfoxide (DMSO-*d6*), chloroform ($CHCl_3$), methanol (MeOH), lithium bromide (LiBr) and 7-mercapto-4-methylcoumarin (≥97.0%) were acquired from Sigma Aldrich and used as received. Biodegradable poly(lactic acid) (PLA) was supplied by NatureWorks® (USA) under the trade name PLA6202D, with <2% of D-lactic acid monomer and a weight-average molecular weight (M_w) of 157.5 kDa.

2.2. Synthesis of poly(mannitol sebacate) and posterior acrylation

Synthesis of PMS was carried out with sebacic acid and D-mannitol in bulk; SA and MA were reacted in a molar ratio 1/1.1 in a 250 mL three-necked round-bottom flask. The temperature was slowly increased to 150 ºC under continuous stirring and nitrogen flow and the reaction was lasted for 7 h. The resulting polymer was dissolved in DMF (150 mg/mL), filtered and purified by dropwise precipitation into a fourfold excess of cold ultrapure water under continuous stirring. The precipitate was collected and dried under vacuum until constant weight.

The obtained polymer was dissolved at 50 mg/mL (5% w/v) in anhydrous DMF under nitrogen flow in a three neck round-bottom flask. The solution was cooled to 0 ºC and acrylation was performed by slowly dropping molar equivalents (768 mM) of TEA and acryloyl chloride into the reaction. The mixture was stirred for 24 h at room temperature. After, ethyl acetate was added to the reaction and vacuum-filtered to remove TEA salt. The process was repeated until a clear solution was obtained. Ethyl acetate was removed by rotary evaporation and the resulting viscous mixture was precipitated into a hydrochloric acid solution (32 mM). Afterwards, the aqueous medium was decanted; the solid was subsequently washed with HCl solution and dried with magnesium sulphate. The obtained functionalized PMS (PMSAc) was protected from light and stored cold until further use (see Scheme 1).

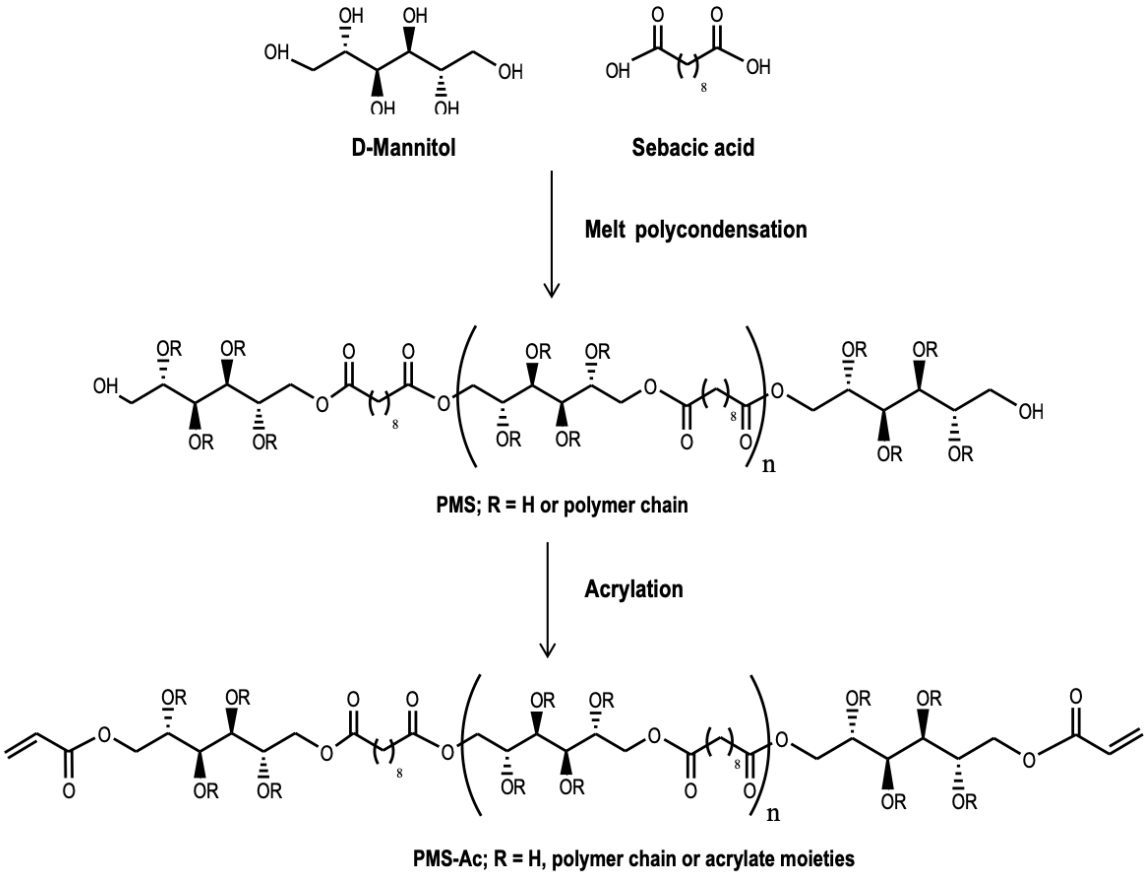

Scheme 1. Synthesis of PMS and its functionalization to synthesize PMSAc.

2.3. Fibers preparation

The electrospinning solutions were prepared from a mixture of PLA and PMS or PMSAc using a ratio of 90/10 wt%, and dissolved in $CHCl_3$/DMF 90:10 (v/v). The solutions were kept under magnetic stirring for 24 h at room temperature to complete homogenization.

Electrospun polymeric fibers were prepared using a home-made electrospinner equipped with a syringe needle connected to a high voltage power supply with horizontal configuration. The prepared solutions were transferred into a syringe and loaded into a pump, placed parallel to the ground, programmed to deliver the solution at constant flow. To promote the collection of the fibers, a rotating drum was used. The employed electrospinning parameters were 16 kV, needle-to-collector distance 12 cm, feeding rate of 1 mL/h and rotor velocity of 1300 rpm. The electrospinning process was carried out at room temperature and the relative humidity was around 30%. The obtained non-woven mats were vacuum dried at room temperature for 24 h to remove any possible solvent residues. Electrospun fibers from pure PLA were also prepared to compare with those loaded with PMS or PMSAc.

2.4. Surface functionalization of fibers

Thiol-ene chemistry was employed to functionalize the electrospun fibers loaded with PMSAc and demonstrate the accessibility of the acrylate groups at the surface. Fiber mats (1x1 cm^2) were incubated in 4 mL of a methanol solution containing 7-mercapto-4-methylcoumarin (0.004 mmol) and trimethylamine (0.016 mmol) at room temperature. After 72 h, the samples were washed with methanol several times to remove any residual reagent and dried.

2.5. Characterization techniques

The number-average molecular weight (M_n), and dispersity (Đ) of PMS were determined by size exclusion chromatography (SEC) using a chromatographic system (Waters Division Millipore) equipped with a Waters model 410 refractive-index detector using N,N-dimethylformamide (Scharlau, 99.9%) containing 0.1% of LiBr as the eluent at a flow rate of 1 mL/min at 50 ºC. Poly(methyl methacrylate) standards (Polymer Laboratories Ltd., Church Stretton, UK) were used to calibrate the system. PMS and PMSAc were characterized by proton and carbon nuclear magnetic resonance spectroscopy (^{1}H- and ^{13}C NMR) using a TM Bruker DPX 400 (400 MHz) spectrometer at room temperature (128 scans, 1 second relaxation delay). Fourier-transform infrared (FTIR) spectra were recorded on a Bruker Alpha instrument with Universal Attenuated Total Reflectance (ATR) sampling accessory module. Theoretical depth penetration of ATR-FTIR is 2.01 μm (Diamond crystal, refractive index: 2.4 and angle of incidence: 45º) and spectral resolution is 0.4 cm^{-1}. Electrospun fibers were characterized by scanning electron microscopy (SEM) using Philips XL30 microscope. The orientation and diameter size were determined from SEM images using Image J software. The thermal behavior of electrospun fibers was analyzed by differential scanning calorimetry (DSC) using a TA Q2000 instrument (TA Instruments) under dry nitrogen (50 cm^3/min). The samples were equilibrated at -60 °C and heated to 200 °C at 10 °C/min. The glass transition temperatures (T_g), cold crystallization temperatures (T_{cc}), melting temperatures (T_m), and the melting enthalpy (ΔH_m) were obtained from the first heating scan. The crystallinity values were obtained by subtracting the enthalpy of crystallization (ΔH_c) from the melting enthalpy (ΔH_m) and dividing it by the melting enthalpy corresponding to a single PLA crystal (ΔH_m^0, perfect crystal = 93.1 J/g) [27]. Errors in the temperature determination, enthalpy calculation, and the crystallinity were estimated at ± 0.5 ºC, ± 4 J/g, and ± 0.04 units, respectively.

The crystalline character of fibers was analyzed by wide angle X-ray diffraction (WAXS) employing synchrotron radiation at the beamline BL11-NCD-SWEET at ALBA (Cerdanyola del Vallés, Barcelona, Spain) at a fixed wavelength of 0.1 nm. A Rayonix detector was used for the WAXS (at about 14.6 cm from sample, and a tilt angle of around 29 degrees) experiments. The spacing calibration was determined by silver behenate and Cr_2O_3 standards. The initial 2D X-ray images were converted into 1D diffractograms as function of the inverse scattering vector, $s = 1/d = 2 \sin \theta/\lambda$, using pyFAI python code (ESRF) that had been modified by the ALBA beamline staff. The mechanical properties

were analyzed using a tensile (stretching) stage from Linkam (model TST350). At least ten rectangular samples were tested for each measurement. Errors in the determination of Young modulus (E) and elongation at break (ε) were estimated as standard deviation.

Surface functionalization of the fibers with coumarin was studied by UV/vis absorption and fluorescence spectra recorded using PerkinElmer Lambda-35 and PerkinElmer LS5OB spectrophotometers, respectively. The surfaces of the fiber mats were also observed with a fluorescence microscope (Nikon Eclipse TE2000-5) combined with a digital Nikon DS-Ri2 camera.

3. Results and Discussion

The synthesis of PMS from sebacic acid and D-mannitol in bulk was successfully performed leading to a polymer with low molecular weight. M_n and Đ obtained by SEC were found to be 2480 g/mol and 1.22, respectively. This low molecular weight is, in principal, ideal for polymer additivation. The chemical composition of PMS polymer was determined via ^{1}H-NMR, by calculating the ratio of sebacic acid to mannitol signal integrals, and obtaining an experimental SA/MA composition of nearly initial stoichiometric value. Peaks from mannitol appeared at 3.5-5.5 ppm due to central and terminal methylene unit while protons from methylene units of sebacic acid appeared at 1.3, 1.6 and 2.3 ppm (see Figure 1). The PMS polymer was subsequently modified by incorporation of acrylate groups in its structures through the hydroxyl groups. The acrylation degree was obtained by comparing the signal intensity of the methylene groups on the sebacic acid backbone (1.3 ppm) to the signal intensity of the acrylate groups (see Figure 1); the resulting value was found to be 87 ± 1% of acrylation degree.

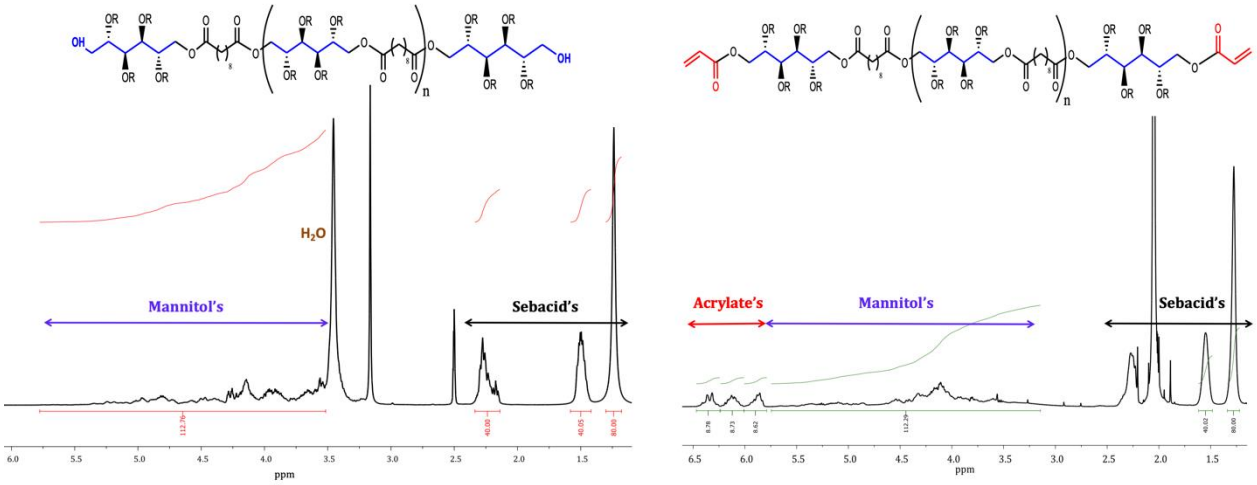

Figure 1. ^{1}H-NMR spectra of synthesized PMS and PMSAc.

Figure 2 shows the ATR-FTIR spectra of PMS and PMSAc. Regarding the PMS spectra, the presence of the band 1740 cm^{-1} also confirms the esterification reaction between mannitol and sebacic acid. Characteristic broad peak around 3470 cm^{-1} associated to the hydroxyl stretch in PMS, lower its intensity in PMSAc spectra after acrylation reaction which also confirms the modification of some hydroxyl moieties from mannitol backbone. In addition to this, bands at 2924 cm^{-1} and 2851 cm^{-1} observed in both PMS and PMSAc correspond to methyl and alkane groups, while the ones shown at 1291-1050 cm^{-1} are associated to the stretching of carboxyl bonds. Peaks associated with acrylate group are seen at 808 cm^{-1} (C=CH$_2$ twisting), 1407 cm^{-1} (C=CH$_2$ scissoring) and 1636 cm^{-1} (C=CH$_2$ stretching). These peaks are absent in PMS polymer.

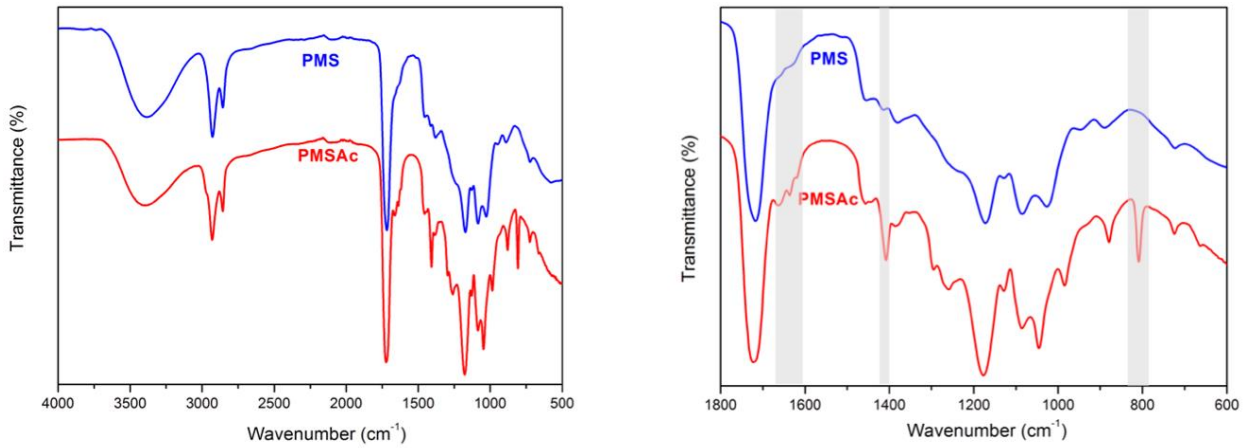

Figure 2. Right side: Complete ATR-FTIR spectra of PMS and PMSAc. Left side: magnified view in the 1800-600 cm^{-1} region.

Then, both synthesized polymers, PMS and PMSAc, were incorporated into PLA electrospinning solutions for the preparation of polymer blend fibers. SEM images of electrospun fibers of neat PLA and blends with PMS and PMSAc are displayed in Figure 3. As observed from the figure the size of the fibers is maintained with the incorporation of PMS and PMSAc with an average value of 3 μm. It is worth mentioning that the rotatory collector clearly induces alignment of PLA fibers in the rotatory collector direction. When PMS and PMSAc are incorporated to the PLA the alignment is slightly altered, going from 90º for PLA to 95 and 92º, for fibers loaded with PMS and PMSAc, respectively, as observed from Figure 3. But there is still a significant alignment in PLA-PMS based fibers. The alignment of nanofibers contributes to the promotion of their applicability in the biomedical field. In particular, aligned nanofibers are potential candidates to be used in wound healing applications since they mimic the extracellular matrix.[28][3] Moreover, it has been demonstrated that an increased alignment of nanofibers can improve cell viability compared to the random fibers [12].

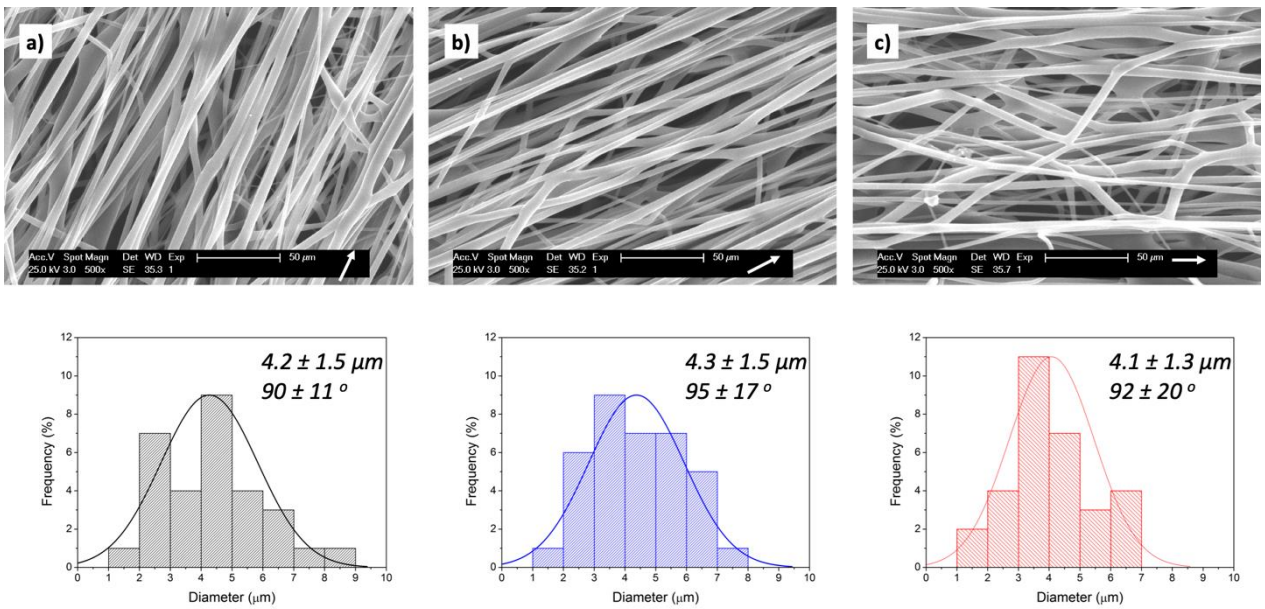

Figure 3. SEM images of electrospun fibers and the corresponding size histograms and orientation of (a) PLA; (b) PLA/PMS and (c) PLA/PMSAc. (White arrows indicate the orientation of the rotatory collector).

In the case of PLA fibers, the uniaxial alignment has also impact in the mechanical properties which improve significantly compared to random ones. Besides of this, the alignment can also promote the development of crystalline structures (α'-, β-) [29] as will be further described.

In order to confirm the composition of the electrospun fibers, in Figure 4 ATR-FTIR spectra of PLA, PLA/PMS and PLA/PMSAc electrospun fibers are shown. In the spectrum corresponding to PLA fibers, the stretching vibration of C=O group is observed at 1750 cm^{-1}; bands at 1450 and 1360 cm^{-1} are attributed to symmetric and asymmetric bending of methyl groups, and at 1380 cm^{-1} to the –CH deformation. At 1185 and 1085 cm^{-1} the symmetric ester -C-O stretching band and -C-O-C asymmetric stretching band can be observed, respectively.

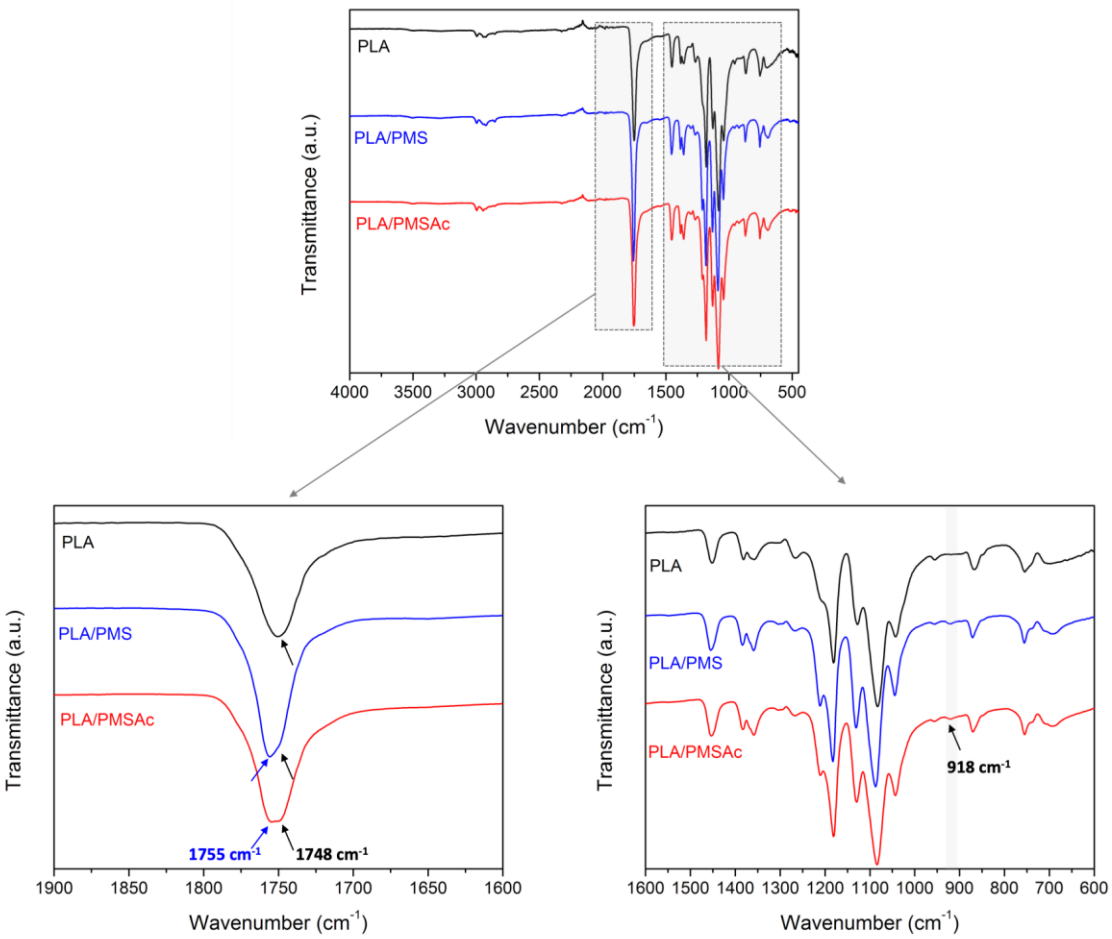

Figure 4. ATR-FTIR spectra of electrospun fibers in the region of 1800-600 cm^{-1}.

The introduction of PMSs slightly modified the PLA spectrum; For instance, changes in the stretching vibration of C=O group are observed showing the presence of a newband at 1755 cm^{-1} associated with the incorporation of PMS and PMSAc (Figure 2). Besides of this, a new band appears at 918 cm^{-1} as highlighted in the figure, which is associated to the development of a crystalline structure, in particular, α form due to the incorporation of PMS and PMSAc. This result is also confirmed by XRD and further explained below.

PLA has polymorphism with four different crystal forms (named α-, β-, γ-, and ε-forms) and two dis-ordered modifications of the α-form (named α′ and α″). It is known that the physical properties of polymers are strongly affected by crystal polymorphism; therefore, the analysis of obtained PLA fibers is essential for understanding their behavior. Figure 5 displays the corresponding WAXS profiles of electrospun fibers at room temperature. The use of synchrotron radiation has allowed detecting small peaks, imperceptible

with CuKα radiation. PLA fibers pattern reveals its amorphous character, presenting very low crystallinity, almost imperceptible. This is also the case of PLA/PMS blend fibers; however, in the blend fibers with PMSAc, the crystallinity starts to appear with visible reflections.

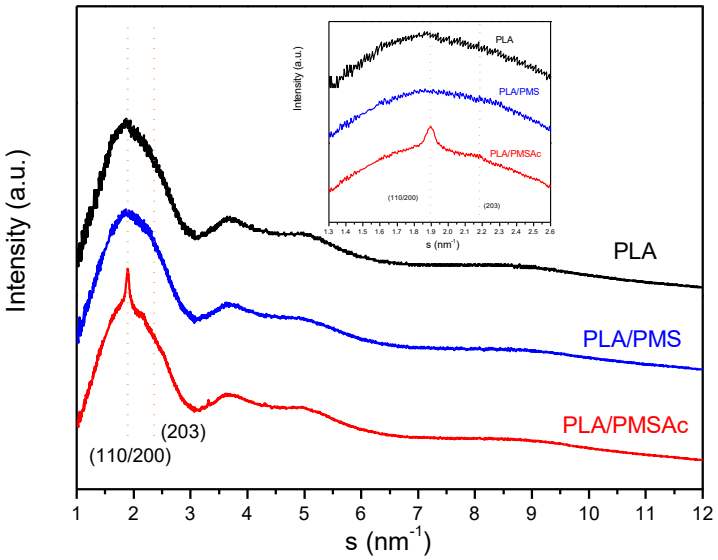

Figure 5. Wide angle X-ray diffraction patterns of PLA, PLA/PMS and PLA/PMSAc fibers.

The α-form of PLA, a pseudo-orthorhombic structure with each unit cell containing two 10_3 helical chains, presents similar chain conformation than in the α' form but in this case more disordered. In the pattern, it can be distinguished a clear reflection at 1.86 nm^{-1} (110/200) and diffuse (203) at 2.12 nm^{-1}, which can be attributed to both forms. The α-form is obtained by isothermal crystallization above 120 °C or by stretching a solution-spun PLA fiber at relatively low drawing temperatures and/or low hot-draw ratios [30]. The α'-form crystals are developed by melt or cold crystallization at lower temperatures (below 100 °C), and a mixture of α-and α'-form crystals is formed in the intermediate temperature region between 100 and 120 °C [31,32]. The diffraction profiles of α and α' forms are quite different at q values >15 nm^{-1} [33,34]. In the present work, crystalline fractions do not allow to distinguish between forms.

Following, the thermal analysis of the samples was performed to determine the corresponding thermal transitions in the electrospun fibers. In Figure 6, it is observed the glass transition temperature (T_g) of PLA, which presents physical aging; subsequently, the cold crystallization process starts followed by the melting of crystalline units. It is clear that there are some recrystallization phenomena occurring as soon as PLA begins to melt and that the beginning of melting starts just after the cold crystallization peak [34,35]. D-lactic acid percentage in the PLA chain influences the melting process and the ratio between α-and α'-forms, which is the current case with 2% of D-lactide in the PLA.

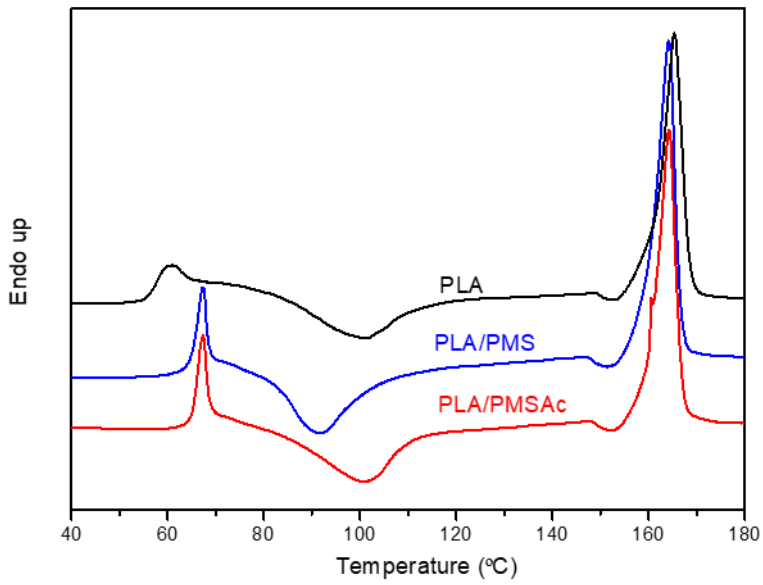

Figure 6. DSC curves of the different electrospun fibers.

It shows similar characteristic parameters as reported in the literature [35–38]. The incorporation of PMS and PMSAc in the fibers slightly changes this behavior. The T_g values of blends are higher than that of neat PLA (see Table 1). This fact could be attributed to the inter- and/or intramolecular hydrogen bonding between PLA and PMSs. The PLA/PMS fibers also start their cold crystallization at lower temperature as well as the melting. However, and although T_m is similar, T_{cc} increases up to PLA values when acrylated PMS is incorporated in the blend. Moreover, the estimation of crystallinity degree by DSC clearly confirms the observed in WAXS measurements. In addition to this, the presence of endothermic peak close to 155 °C present in each sample is also indicative of the presence of α'-form [34].

Table 1. Thermal parameters obtained from the different fibers.

Fibers	T_g (ºC)	T_{cc} (ºC)	ΔH_{cc} (J/g)	T_m (ºC)	ΔH_m (J/g)	X_c (%)
PLA	60	101	32	165	37	5
PLA/PMS	67	92	33	164	39	6
PLA/PMSAc	67	101	33	164	41	9

Then, the mechanical properties of all obtained fibers were analyzed by uniaxial tensile experiments at room temperature tested at 10 mm/min stretching rate. Figure 7 depicts the representative profiles of the stress-strain curves of the obtained fibers and Table 2 collects the corresponding Young modulus and elongation at break. It is worthy to remark that the reached E values are attributed to the fiber alignment as it was mentioned before. As can be clearly observed, the incorporation of only 10 wt% of PMS or PMSAc to PLA fibers makes the system more ductile, due to the elastomeric features of PMS. The elongation at break (ε) increases whereas the tensile strength (σ_{max}) and the Young modulus (E) decrease in comparison with PLA fibers. In PLA fibers typically a necking is produced before the fracture, herein the incorporation of PMSs avoids this and the strength is maintained before fracture. The fibers with the unmodified PMS almost duplicate its strain capacity, and in the case of PMSAc this behavior is even more pronounced. The high value of elongation at break in fibers loaded with PMSAc could be attributed to modifications on the hydrogen bonding (intra and intermolecular) interactions due to the acrylation reaction.

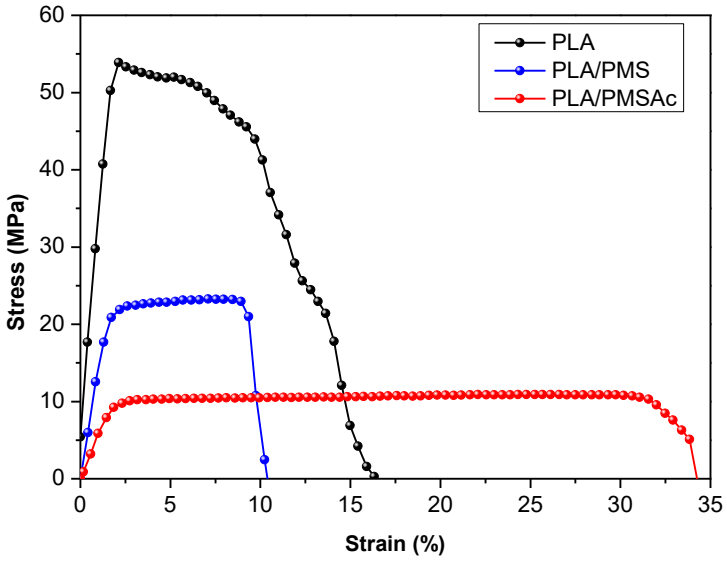

Figure 7. Stress-stain curves of electrospun fibers of PLA, PLA/PMS and PLA/PMSAc at 10 mm/min.

Table 2. Mechanical parameters obtained from the different fibers.

Fibers	E (GPa)	σ_{max} (MPa)	ε (%)
PLA	2.2 ± 0.4	38 ± 8	8 ± 3
PLA/PMS	1.2 ± 0.2	31 ± 3	14 ± 2
PLA/PMSAc	0.8 ± 0.1	13 ± 4	31 ± 6

Therefore, the incorporation of low percentage of this PMSAc polymer seems to be a promising alternative to improve the ability of the material to bend and deform. Furthermore, PMSAc presents reactive acrylate groups which also confer surface activity to the fibers, and includes the potential for further chemical modification on the surface such as grafting, crosslinking or thiol-ene click chemistry reactions. The thiol-ene Michael addition between a thiol and activated vinyl group such as acrylate is a fast, high efficient and metal catalyst free conjugation approach for the covalent attachment of functional compounds to surfaces in mild conditions [39][40][41]. To study the accessibility of the acrylate functional groups at the surface of the fibers, a Michael addition between the activated acrylate groups of PMSAc at the fiber surface and a mercapto-coumarin, used as fluorescent probe, was carried out in the presence of triethylamine as catalyst at ambient temperature (Figure 8a). The surface reaction was successfully performed in mild conditions and tested by fluorescence microscopy and spectroscopy (Figures 8b, c and d).

As shown in Figure 8, the PLA/PMSAc fibers containing available acrylate groups showed strong fluorescence after the attachment of the thiol functional dye, whereas the PLA/PMS fibers used as control, showed no fluorescence. Therefore, it is confirmed the successful modification of the PLA/PMSAc fiber surface.

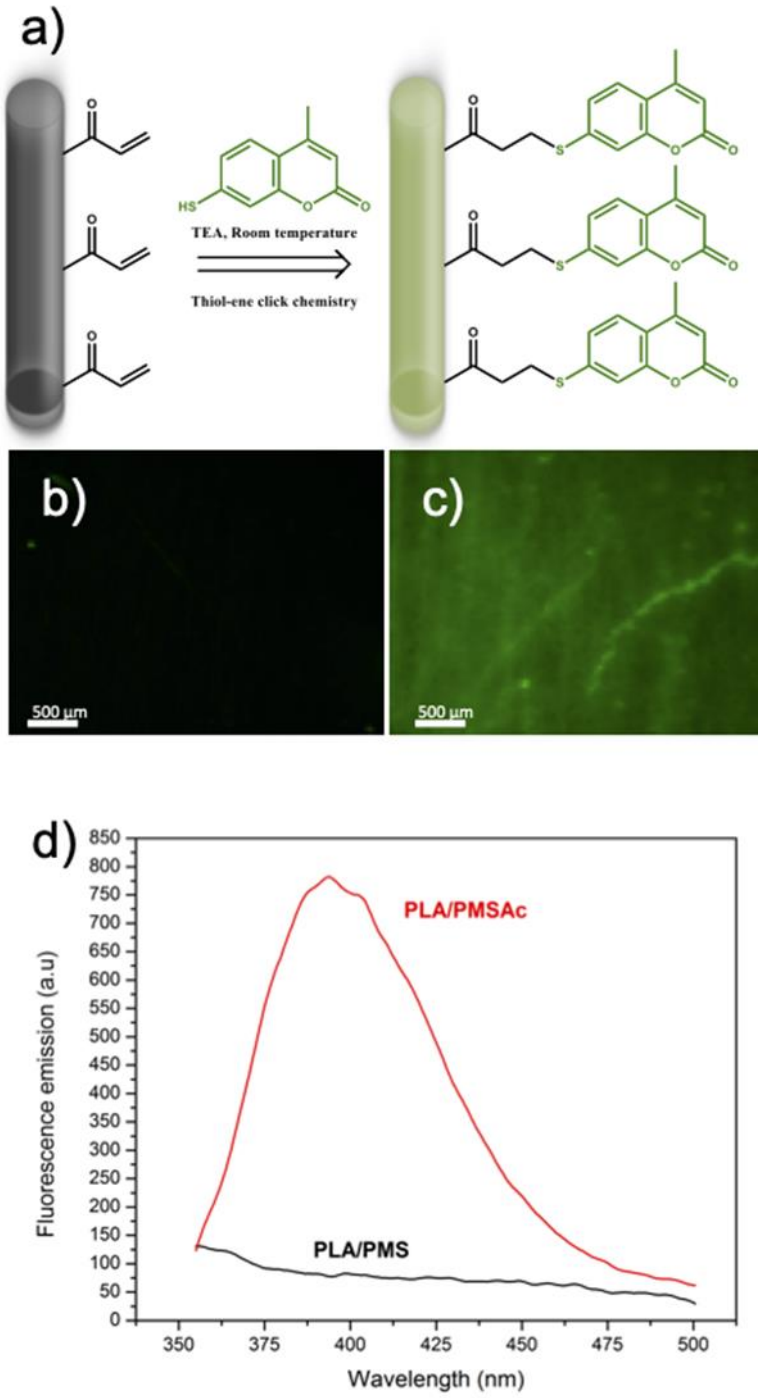

Figure 8. a) Schematic illustration for the preparation process of fibers surface modification with thiol-ene click chemistry. b) and c) Fluorescence micrographs of PLA/PMS and PLA/PMSAc fibers, respectively, after thiol-ene reaction with mercapto-coumarin taken under the same exposure time. d) Fluorescence espectra PLA/PMS and PLA/PMSAc fibers, respectively, after thiol-ene reaction with mercapto-coumarin using an excitation wavelength of 325 nm.

4. Conclusions

In summary, this work described the synthesis of biobased PMS and vinyl functionalized PMS, to be used as components of PLA based elecrospun fibers with the purpose of enhancing their mechanical properties. Partially aligned fibers containing 90% of PLA and 10% of the resulting low molecular weight PMS or PMSAc were successfully obtained by electrospinning. These fibers present low degree of crystallinity as demonstrated by

WAXS and DSC measurements, although the incorporation of PMS and PMSAc slightly increases the crystallinity and augments the T_g of the samples. Remarkably, the elasticity of PLA based fibers was enhanced with the addition of the low amount of PMS or PMSAc, while the maximum strength reached was retained without a sudden drop before fracture in contrast with what occurs in neat PLA fibers. These phenomena occur more markedly in PLA/PMSAc fibers, and in addition, the acrylated polyester also presents the possibility for further functionalization through the vinyl groups, which was demonstrated by the attachment of a thiol functional dye via Michael addition at the surface of the PLA based fibers. Therefore, the incorporation of PMSAc at low amount in PLA based fibers enhanced their elasticity and toughness, and also provided functional groups at the surface available for further chemical modification such as grafting, crosslinking or bioconjungation through chemistry reactions.

Funding: This work was funded by the MICINN (project PID2019-104600RB-I00) and by the Valencian Autonomous Government, Generalitat Valenciana, GVA (GV/2021/182).

Acknowledgments: The synchrotron experiments were performed at beamlines BL11-NCD-SWEET and MIRAS at ALBA Synchrotron Light Facility and authors would like to thank the help of ALBA staff. Authors also thank M.L. Cerrada for her invaluable discussions on crystallinity. Authors thank T.M. Díez-Rodríguez and E. Blázquez-Blázquez for conducting some tests. A. S. acknowledges her "APOSTD/2018/228" and "PAID-10-19" postdoctoral contracts from the Education, Research, Culture and Sport Council from the Government of Valencia and from the Polytechnic University of Valencia, respectively.

Conflicts of Interest: The authors declare no conflict of interest.

References

1. Agarwal, S.; Greiner, A.; Wendorff, J.H. Functional materials by electrospinning of polymers. *Prog. Polym. Sci.* **2013**, *38*, 963–991, doi:10.1016/J.PROGPOLYMSCI.2013.02.001.
2. Xu, Q.; Gao, X.; Zhao, S.; Liu, Y.N.; Zhang, D.; Zhou, K.; Khanbareh, H.; Chen, W.; Zhang, Y.; Bowen, C. Construction of Bio-Piezoelectric Platforms: From Structures and Synthesis to Applications. *Adv. Mater.* **2021**, *33*, doi:10.1002/adma.202008452.
3. Xie, X.; Chen, Y.; Wang, X.; Xu, X.; Shen, Y.; Khan, A. ur R.; Aldalbahi, A.; Fetz, A.E.; Bowlin, G.L.; El-Newehy, M.; et al. Electrospinning nanofiber scaffolds for soft and hard tissue regeneration. *J. Mater. Sci. Technol.* **2020**, *59*, 243–261, doi:10.1016/j.jmst.2020.04.037.
4. Dutta, R.C.; Dey, M.; Dutta, A.K.; Basu, B. Competent processing techniques for scaffolds in tissue engineering. *Biotechnol. Adv.* **2017**, *35*, 240–250, doi:10.1016/j.biotechadv.2017.01.001.
5. Xue, J.; Wu, T.; Dai, Y.; Xia, Y. Electrospinning and electrospun nanofibers: Methods, materials, and applications. *Chem. Rev.* **2019**, *119*, 5298–5415, doi:10.1021/acs.chemrev.8b00593.
6. Rahmani, M.; Faridi-Majidi, R.; Khani, M.M.; Mashaghi, A.; Noorizadeh, F.; Ghanbari, H. Cross-linked PMS/PLA nanofibers with tunable mechanical properties and degradation rate for biomedical applications. *Eur. Polym. J.* **2020**, *130*, 109633, doi:10.1016/j.eurpolymj.2020.109633.
7. Bhattacharya, S.; Roy, I.; Tice, A.; Chapman, C.; Udangawa, R.; Chakrapani, V.; Plawsky, J.L.; Linhardt, R.J. High-Conductivity and High-Capacitance Electrospun Fibers for Supercapacitor Applications. *ACS Appl. Mater. Interfaces* **2020**, *12*, 19369–19376, doi:10.1021/ACSAMI.9B21696/ASSET/IMAGES/LARGE/AM9B21696_0003.JPEG.
8. Luo, B.; Tian, L.; Chen, N.; Ramakrishna, S.; Thakor, N.; Yang, I.H. Electrospun nanofibers facilitate better alignment, differentiation, and long-term culture in an: In vitro model of the neuromuscular junction (NMJ). *Biomater. Sci.* **2018**, *6*, 3262–3272, doi:10.1039/c8bm00720a.
9. Wang, Y.; Jiang, Y.; Zhang, Y.; Wen, S.; Wang, Y.; Zhang, H. Dual functional electrospun core-shell nanofibers for anti-infective guided bone regeneration membranes. *Mater. Sci. Eng. C* **2019**, *98*, 134–139, doi:https://doi.org/10.1016/j.msec.2018.12.115.
10. Flaig, F.; Ragot, H.; Simon, A.; Revet, G.; Kitsara, M.; Kitasato, L.; Hébraud, A.; Agbulut, O.; Schlatter, G. Design of Functional Electrospun Scaffolds Based on Poly(glycerol sebacate) Elastomer and Poly(lactic acid) for Cardiac Tissue Engineering. *ACS Biomater. Sci. Eng.* **2020**, *6*, 2388–2400, doi:10.1021/acsbiomaterials.0c00243.
11. Yang, J.; Wang, K.; Yu, D.-G.; Yang, Y.; Bligh, S.W.A.; Williams, G.R. Electrospun Janus nanofibers loaded with a drug and inorganic nanoparticles as an effective antibacterial wound dressing. *Mater. Sci. Eng. C* **2020**, *111*, 110805, doi:https://doi.org/10.1016/j.msec.2020.110805.
12. Rezvani Ghomi, E.; Khosravi, F.; Neisiany, R.E.; Shakiba, M.; Zare, M.; Lakshminarayanan, R.; Chellappan, V.; Abdouss, M.; Ramakrishna, S. Advances in electrospinning of aligned nanofiber scaffolds used for wound dressings. *Curr. Opin. Biomed. Eng.* **2022**, *22*, 100393, doi:10.1016/j.cobme.2022.100393.

13. Saini, P.; Arora, M.; Kumar, M.N.V.R. Poly(lactic acid) blends in biomedical applications. *Adv. Drug Deliv. Rev.* **2016**, *107*, 47–59, doi:https://doi.org/10.1016/j.addr.2016.06.014.
14. Rahmani, M.; Khani, M.M.; Rabbani, S.; Mashaghi, A.; Noorizadeh, F.; Faridi-Majidi, R.; Ghanbari, H. Development of poly (mannitol sebacate)/poly (lactic acid) nanofibrous scaffolds with potential applications in tissue engineering. *Mater. Sci. Eng. C* **2020**, *110*, 110626, doi:10.1016/j.msec.2020.110626.
15. Aragón-Gutierrez, A.; Arrieta, M.P.; López-González, M.; Fernández-García, M.; López, D. Hybrid biocomposites based on poly(Lactic acid) and silica aerogel for food packaging applications. *Materials (Basel).* **2020**, *13*, doi:10.3390/ma13214910.
16. Nazrin, A.; Sapuan, S.M.; Zuhri, M.Y.M.; Ilyas, R.A.; Syafiq, R.; Sherwani, S.F.K. Nanocellulose Reinforced Thermoplastic Starch (TPS), Polylactic Acid (PLA), and Polybutylene Succinate (PBS) for Food Packaging Applications. *Front. Chem.* **2020**, *8*, 1–12, doi:10.3389/fchem.2020.00213.
17. Sonseca, A.; Madani, S.; Rodriguez, G.; Hevilla, V.; Echeverria, C.; Fernandez-Garcia, M.; Munoz-Bonilla, A.; Charef, N.; Lopez, D. Multifunctional PLA Blends Containing Chitosan Mediated Silver Nanoparticles: Thermal, Mechanical, Antibacterial, and Degradation Properties. *Nanomater.* **2019**, *10*, doi:10.3390/nano10010022.
18. Rosli, N.A.; Karamanlioglu, M.; Kargarzadeh, H.; Ahmad, I. Comprehensive exploration of natural degradation of poly(lactic acid) blends in various degradation media: A review. *Int. J. Biol. Macromol.* **2021**, *187*, 732–741, doi:10.1016/j.ijbiomac.2021.07.196.
19. Lang, K.; Sánchez-Leija, R.J.; Gross, R.A.; Linhardt, R.J. Review on the impact of polyols on the properties of bio-based polyesters. *Polymers (Basel).* 2020, *12*, 1–25. https://doi.org/10.3390/polym12122969
20. Bruggemana, J.P.; Bruina, B.-J. de; Bettingera, C.J.; Langer, R. Biodegradable Poly(polyol sebacate) Polymers. *Biomaterials* **2008**, *29*, 4726–4735, doi:10.1016/j.biomaterials.2008.08.037.Biodegradable.
21. Daniel, W.; Stiriba, S.E.; Holger, F. Hyperbranched polyglycerols: From the controlled synthesis of biocompatible polyether polyols to multipurpose applications. *Acc. Chem. Res.* **2010**, *43*, 129–141, doi:10.1021/ar900158p.
22. Sonseca, Á.; Camarero-Espinosa, S.; Peponi, L.; Weder, C.; Foster, E.J.; Kenny, J.M.; Giménez, E. Mechanical and shape-memory properties of poly(mannitol sebacate)/cellulose nanocrystal nanocomposites. *J. Polym. Sci. Part A Polym. Chem.* **2014**, *52*, 3123–3133, doi:10.1002/pola.27367.
23. Tham, W.H.; Wahit, M.U.; Abdul Kadir, M.R.; Wong, T.W.; Hassan, O. Polyol-based biodegradable polyesters: a short review. *Rev. Chem. Eng.* **2016**, *32*, 201–221, doi:doi:10.1515/revce-2015-0035.
24. Wcisłek, A.; Sonseca Olalla, A.; McClain, A.; Piegat, A.; Sobolewski, P.; Puskas, J.; El Fray, M. Enzymatic Degradation of Poly(butylene succinate) Copolyesters Synthesized with the Use of Candida antarctica Lipase B. *Polymers (Basel).* **2018**, *10*, 688, doi:10.3390/polym10060688.
25. Lee, S.-H.; Sonseca, Á.; Vadrucci, R.; Giménez, E.; Foster, E.J.; Simon, Y.C. Low-Power Upconversion in Poly(Mannitol-Sebacate) Networks with Tethered Diphenylanthracene and Palladium Porphyrin. **2014**, *24*, 1–43.
26. Sonseca, Á.; Sahuquillo, O.; Foster, E.J.; Giménez, E. Mechanical properties and degradation studies of poly(mannitol sebacate)/cellulose nanocrystals nanocomposites. *RSC Adv.* **2015**, *5*, 55879–55891, doi:10.1039/c5ra06768e.
27. Lim, L.T.; Auras, R.; Rubino, M. Processing technologies for poly(lactic acid). *Prog. Polym. Sci.* **2008**, *33*, 820–852, doi:10.1016/j.progpolymsci.2008.05.004.
28. Chen, Y.; Dong, X.; Shafiq, M.; Myles, G.; Radacsi, N.; Mo, X. Recent Advancements on Three-Dimensional Electrospun Nanofiber Scaffolds for Tissue Engineering. *Adv. Fiber Mater.* **2022**, doi:10.1007/s42765-022-00170-7.
29. Echeverría, C.; Limón, I.; Muñoz-Bonilla, A.; Fernández-García, M.; López, D. Development of highly crystalline polylactic acid with β-crystalline phase from the induced alignment of electrospun fibers. *Polymers (Basel).* **2021**, *13*, doi:10.3390/polym13172860.
30. Zhou, C.; Li, H.; Zhang, W.; Li, J.; Huang, S.; Meng, Y.; De Claville Christiansen, J.; Yu, D.; Wu, Z.; Jiang, S. Thermal strain-induced cold crystallization of amorphous poly(lactic acid). *CrystEngComm* **2016**, *18*, 3237–3246, doi:10.1039/c6ce00464d.
31. Zhang, J.; Tashiro, K.; Tsuji, H.; Domb, A.J. Disorder-to-order phase transition and multiple melting behavior of poly(L-lactide) investigated by simultaneous measurements of WAXD and DSC. *Macromolecules* **2008**, *41*, 1352–1357, doi:10.1021/ma0706071.
32. Marubayashi, H.; Asai, S.; Hikima, T.; Takata, M.; Iwata, T. Biobased copolymers composed of l -lactic acid and side-chain-substituted lactic acids: Synthesis, properties, and solid-state structure. *Macromol. Chem. Phys.* **2013**, *214*, 2546–2561, doi:10.1002/macp.201300406.
33. Wasanasuk, K.; Tashiro, K.; Hanesaka, M.; Ohhara, T.; Kurihara, K.; Kuroki, R.; Tamada, T.; Ozeki, T.; Kanamoto, T. Crystal structure analysis of poly(l-lactic acid) α form on the basis of the 2-dimensional wide-angle synchrotron X-ray and neutron diffraction measurements. *Macromolecules* **2011**, *44*, 6441–6452, doi:10.1021/ma2006624.
34. Hsieh, Y.T.; Nozaki, S.; Kido, M.; Kamitani, K.; Kojio, K.; Takahara, A. Crystal polymorphism of polylactide and its composites by X-ray diffraction study. *Polym. J.* **2020**, *52*, 755–763, doi:10.1038/s41428-020-0343-8.
35. Díez-Rodríguez, T.M.; Blázquez-Blázquez, E.; Pérez, E.; Cerrada, M.L. Composites based on poly(Lactic acid) (pla) and sba-15: Effect of mesoporous silica on thermal stability and on isothermal crystallization from either glass or molten state. *Polymers (Basel).* **2020**, *12*, 1–22, doi:10.3390/polym12112743.
36. Arrieta, M.P.; Peponi, L.; López, D.; Fernández-García, M. Recovery of yerba mate (Ilex paraguariensis) residue for the development of PLA-based bionanocomposite films. *Ind. Crops Prod.* **2018**, *111*, doi:10.1016/j.indcrop.2017.10.042.
37. Leonés, A.; Salaris, V.; Mujica-Garcia, A.; Arrieta, M.P.; Lopez, D.; Lieblich, M.; Kenny, J.M.; Peponi, L. Pla electrospun fibers reinforced with organic and inorganic nanoparticles: A comparative study. *Molecules* **2021**, *26*, doi:10.3390/molecules26164925.
38. Echeverría, C.; Limón, I.; Muñoz-Bonilla, A.; Fernández-García, M.; López, D. Development of highly crystalline polylactic acid with β-crystalline phase from the induced alignment of electrospun fibers. *Polymers (Basel).* **2021**, *13*, doi:10.3390/polym13172860.

39. Heggli, M.; Tirelli, N.; Zisch, A.; Hubbell, J.A. Michael-type addition as a tool for surface functionalization. *Bioconjug. Chem.* **2003**, *14*, 967–973, doi:10.1021/bc0340621.
40. Mohammad Mahdi Dadfar, S.; Sekula-Neuner, S.; Trouillet, V.; Hirtz, M. A Comparative Study of Thiol-Terminated Surface Modification by Click Reactions: Thiol-yne Coupling versus Thiol-ene Michael Addition. *Adv. Mater. Interfaces* **2018**, *5*, 1–9, doi:10.1002/admi.201801343.
41. Resetco, C.; Hendriks, B.; Badi, N.; Du Prez, F. Thiol-ene chemistry for polymer coatings and surface modification-building in sustainability and performance. *Mater. Horizons* **2017**, *4*, 1041–1053, doi:10.1039/c7mh00488e.